Sensorless Control of AC Machines

Werner Zimmermann
Fachhochschule fuer Technik Esslingen
Flandernstraße 101, D-73732 Esslingen, Germany
EMail: Werner.Zimmermann@fht-esslingen.de

Abstract

Inverter fed AC machines are used in many applications, where high dynamic performance is needed, but position control is not required. Conventional field oriented control fulfills the dynamic requirements, but usually needs a costly position or speed sensor. Simple voltage-frequency-control avoids these sensors, but will only achieve a moderate dynamic performance. For such applications a self controlled scheme based on the measured flux vector may be used. In this paper a flux phase control loop and a method of backing the flux model with an observer to improve the behaviour at low stator frequencies are described. The flux observer may be easily controlled by signals from the the inverter's current control system, which by using the 'free wheeling state' efficiently reduces the thermal stress of the inverter.

1. Introduction

Modern microelectronics have changed the world of electrical drives, where AC machines seem to have completely conquered the field of speed variable drives, which formerly was a domain of DC machines. With modern power transistors, high performance inverters, pioneered in such applications by Boehringer and others in the late 1970s [1], can be realized at reasonable cost. Today's modern microcontrollers, DSPs (digital signal processors) and ASICs (application specific integrated circuits) allow the implementation of the necessary complicated control structures based on the work of Blaschke, Leonhard et.alt. [2].

With Depenbrock's principle of 'direct self control' (DSC) two remaining problems of the field oriented control could be overcome [3]. DSC reduces the sensivity of the control algorithm to variations of the machine parameters by introducing closed loop flux control and takes into account the limitations of the inverter, i.e. the finite switching states, switching frequency and limited output voltage. Especially this latter feature makes DSC well suited for use in high power traction drives. As a positive side effect, DSC does not inherently need a position sensor.
In this paper a variant of DSC for inverters with underlying current control and squirrel cage AC machines without speed or position sensor is described, which is very well suited for applications, where high dynamic performance is demanded, but position control is not needed and speed accuracy requirements are not extreme.

2. Dynamic behaviour of asynchronous machines

Fig.1 shows simplified equivalent circuits of the asynchronous machine. Fig.1a describes the behaviour of the stator circuit, suited for considering transient effects in stator current control loops.

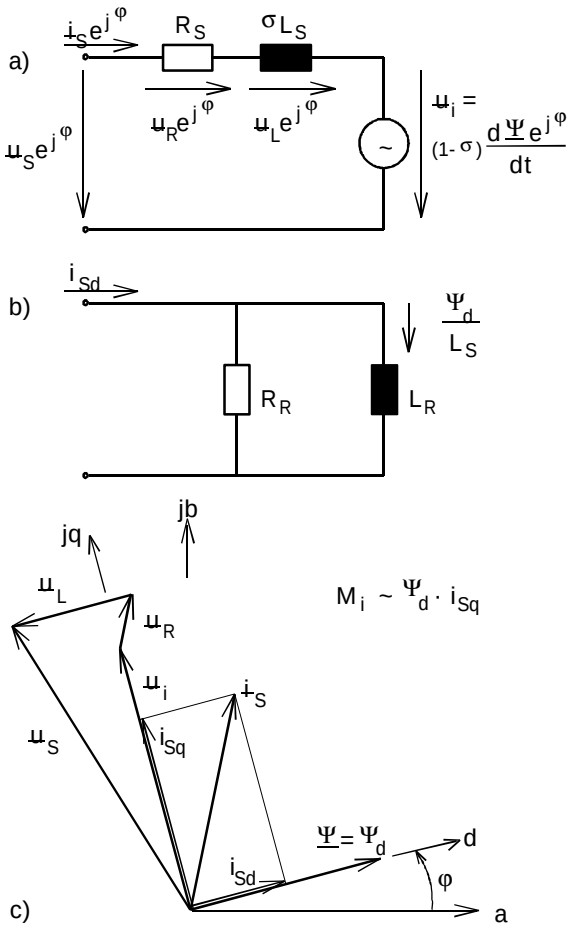

Figure 1: Equivalent circuit of the asynchronous machine a) stator b) rotor c) space vector diagram (abbreviations see appendix A)

The easiest way to control the machine is to apply a stator voltage U_S and frequency $\omega_S=2\pi f_S=d\varphi/dt$ proportional to the desired speed n (Fig.3). This ensures a nearly constant, speed independent magnetization. At low speeds the stator voltages must be slightly increased to compensate for the resistive voltage drops. At high speeds, the stator voltages are held constant to the inverters maximum output value, operating the machine in the field weakening range. Due to the slip, there will be a slight, load dependent deviation of the the machine's speed from the set stator frequency. This can also be compensated for by measuring the amplitude of the stator currents. This control scheme works without a speed sensor, but does only have a moderate dynamic performance. During fast load and speed

changes there may be heavy transient oscillations of the machine's torque, as the phase relations of the currents and voltages are not taken into account.

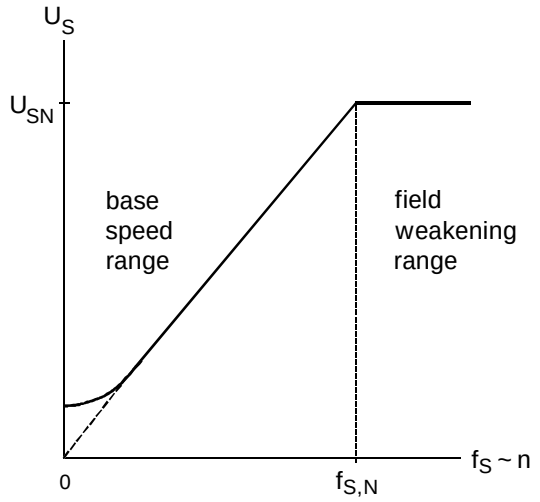

Figure 2: Voltage - frequency control

As can be seen from the space vector diagram in Fig.1c, only that component i_{Sq} of the stator current $\underline{i}_S = i_{Sd} + j\, i_{Sq}$, which is in phase with the voltage $\underline{u}_i$ induced by the flux linkage $\underline{\Psi} = \Psi_d$ (per definition is $\Psi_q = 0$) directly produces mechanical torque M_i. The orthogonal component i_{Sd} controls the magnetic field and thus the amplitude of the flux linkage Ψ_d, shown in the rotor equivalent circuit in Fig.1b. The angle φ describes the angular position of Ψ_d in a stator fixed reference frame a,b (Fig.1c), thus

$$\varphi(t) = \int_0^t \omega_S(\tau) \cdot d\tau \ , \qquad (1)$$

where ω_S is the angular frequency of Ψ_d with respect to the stator (please note: under dynamic operating conditions the angular frequency ω_S of Ψ_d and that of u_S may be different). As the stator transient time constant $T_{S\sigma} = \sigma L_S / R_S$ (Fig.1a) is much smaller than the rotor time constant $T_R = L_R / R_R$ (Fig.1b), the idea of field oriented control is to use i_{Sq} for high dynamic torque control and to hold i_{Sd} and thus Ψ_d constant - at least as long as there is no need for field weakening - to avoid slow transients in the machine's magnetic field.

3. Torque, flux and current control

According to Blaschke's idea the set values of i_{Sq} and i_{Sd} come from a speed controller and a flux controller, respectively, and are transformed into phase current set values $i_{S\nu}^*$ (ν=1,2,3) with stator frequency by a vector modulator (Fig.3). The underlying current control loop consists of simple comparators. The output signals of the comparators are sampled in regular clock intervals and turn the inverter switches on and off.

To reduce the average switching frequency and thus the thermal stress of the inverter without affecting its dynamic behaviour, the machine windings are short circuited (free wheeling state), whenever the magnitude of the current deviation is below a certain limit in all three phases.

3.1 Current control with free wheeling and inverter stress

With this type of current control, the maximum switching frequency of the inverter is $f_{S,max} = 1/2T$, where T is the clock period of the inverter, e.g. 25µs. Due to the thermal capacities, however, the thermal stress of the inverter's semiconductors does not directly depend on the maximum switching frequency, but is more or less proportional to the average switching frequency.

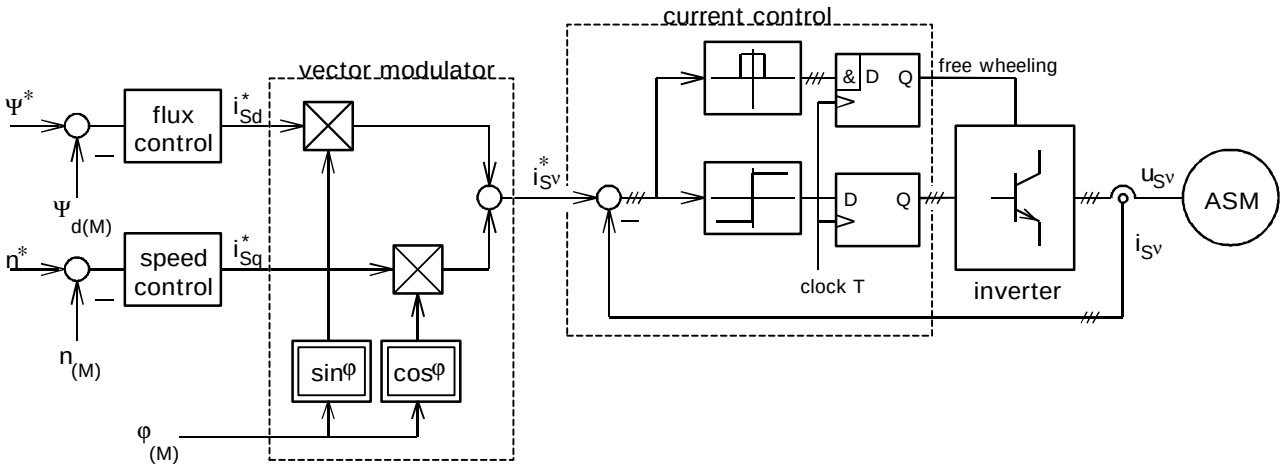

Figure 3: Current, torque (speed) and flux control
ASM ... asynchronous machine * ... set values M ... measured or observed values

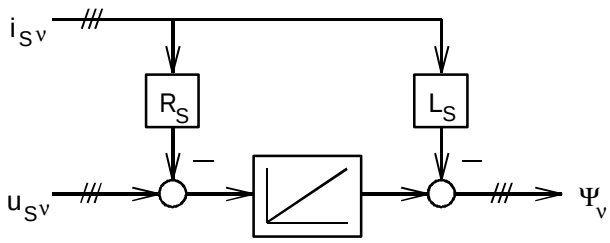

Figure 7: Flux identification measuring Ψ_ν (ν=1,2,3)

As during steady state operation the inverter output currents and the fundamental cycle of the output voltages are sinusoidal, the average may be calculated over a period of the stator frequency. Fig.4 shows the average switching frequency $f_{S,av}$ versus the amplitude of the (fundamental cycle) of the output voltage $\hat{u}_{s0}$. This diagram clearly shows, that the average switching frequency in a system without free wheeling (W I) is much higher than that with free wheeling (W II). The positive effect of using free wheeling states on the switching frequency is achieved without increasing the ripple of the output currents (Fig.5).

However, at very low stator frequencies the thermal time constants of the inverter's semiconductors are nolonger great compared to the period of the stator currents and voltages. In this operating range the thermal stress of the inverter is better described by the peak switching frequency $f_{S,peak}$, which is the average over a small number of switching cycles. As can be seen from Fig.6, at low output voltages the current control with free wheeling (W II) also leads to lower peak switching frequencies. With AC machines low stator frequencies correspond with low voltages. Thus, the current control system with free wheeling ensures a lower stress for the inverter semiconductors in the whole operating range. A more detailled

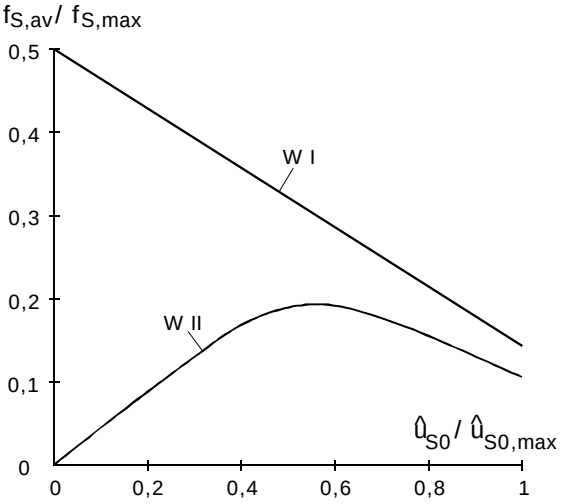

Figure 4: Average inverter switching frequency for current control without (W I) and with (WII) free wheelng

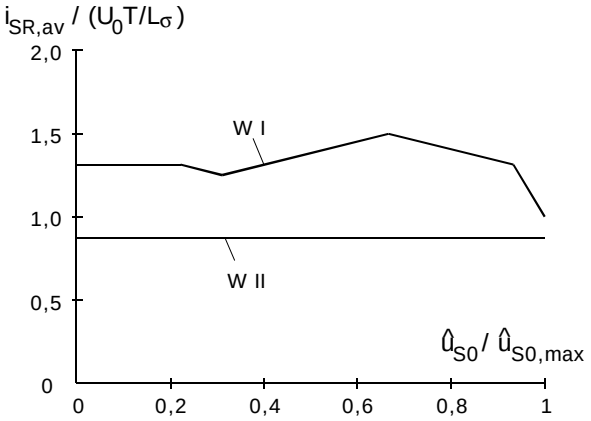

Figure 5: Average current ripple for current control without (W I) and with (W II) free wheeling

description of this control scheme is given in [4,5].

4. Identifying the flux vector

The key in field oriented control lies in identifying the amplitude Ψ_d and the angle φ of the flux. As can be seen in Fig. 1a, it is possible to compute

$$\Psi_\nu(t) = \int_0^t [u_{S\nu}(\tau) - R_S \cdot i_{S\nu}(\tau)] \cdot d\tau - \sigma L_S \cdot i_{S\nu}(t) \qquad (2)$$

by measuring and integrating the voltages and currents $u_{S\nu}$ and $i_{S\nu}$ in the three phases ν=1,2,3 (Fig.7).

From these three signals a quadrature voltage pair with

$$\Psi_a = \Psi_1 = \Psi_d \cdot \cos\varphi(t)$$

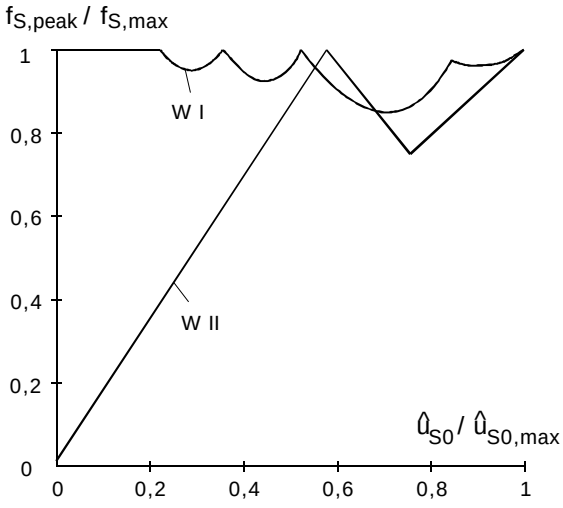

Figure 6: Peak inverter switching frequency for current control without (W I) and with (WII) free wheelng

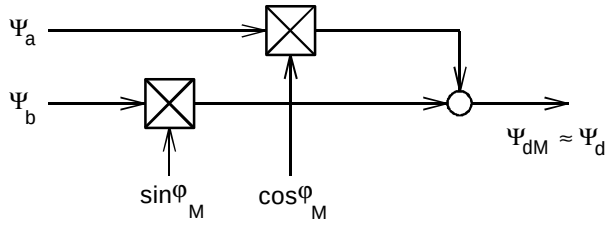

Figure 9: Flux identification by computing Ψ_d

and $$\Psi_b = (\Psi_2 - \Psi_3)/\sqrt{3} = \Psi_d \cdot \sin\varphi(t) \qquad (3)$$

is derived by simple additions (Fig.8). In a second vector modulator these signals are transformed via

$$\begin{aligned}\Psi_{qM} &= -\Psi_a \cdot \sin\varphi_M + \Psi_b \cdot \cos\varphi_M \\ &= \Psi_d \cdot [\cos\varphi(t) \cdot \sin\varphi_M(t) - \sin\varphi(t) \cdot \cos\varphi_M(t)] \\ &= \Psi_d \cdot \sin(\varphi - \varphi_M) \qquad (4)\end{aligned}$$

and fed to a comparator and integrator (Fig.8). If Ψ_{qM} is positive, φ_M is increased, if Ψ_{qM} is negativ, φ_M is decreased. Due to the closed loop configuration the comparator and integrator will enforce

$$\Psi_{qM} \approx 0$$

and thus $$\varphi_M \approx \varphi . \qquad (5)$$

With a third vector modulator $\Psi_{dM} \approx \Psi_d$ is computed (Fig.9). Such vector modulators may be realized combining analog and digital techniques [6] and are now available as integrated circuits [7].

By this phase control loop, the flux angle φ and thus the stator frequency ω_S are self controlled. The resulting stator frequency ω_S may be measured by computing the derivate $d\varphi/dt$ or by low pass filtering the output of the comparator, as shown in Fig. 8.

5. Speed calculation

With asynchronous machines speed n is

$$n \sim (\omega_S - s \cdot \omega_S) \qquad (6a)$$

where

$$s\omega_S = R_R \cdot \frac{L_S}{L_R} \cdot \frac{i_{Sq}}{\Psi_d} \qquad (6b)$$

is the so called slip frequency. For machines above 1kW output power, the slip frequency typically is less than 5% of the stator angular frequency ω_{SN} at nominal speed. Therefore the slip may be neglected at higher speeds. To improve the accuracy of the speed regulation at lower speeds, n may be corrected according to eq. (6). As at low stator frequencies Ψ_d is kept constant, the correction may be linearized as shown in Fig.8.

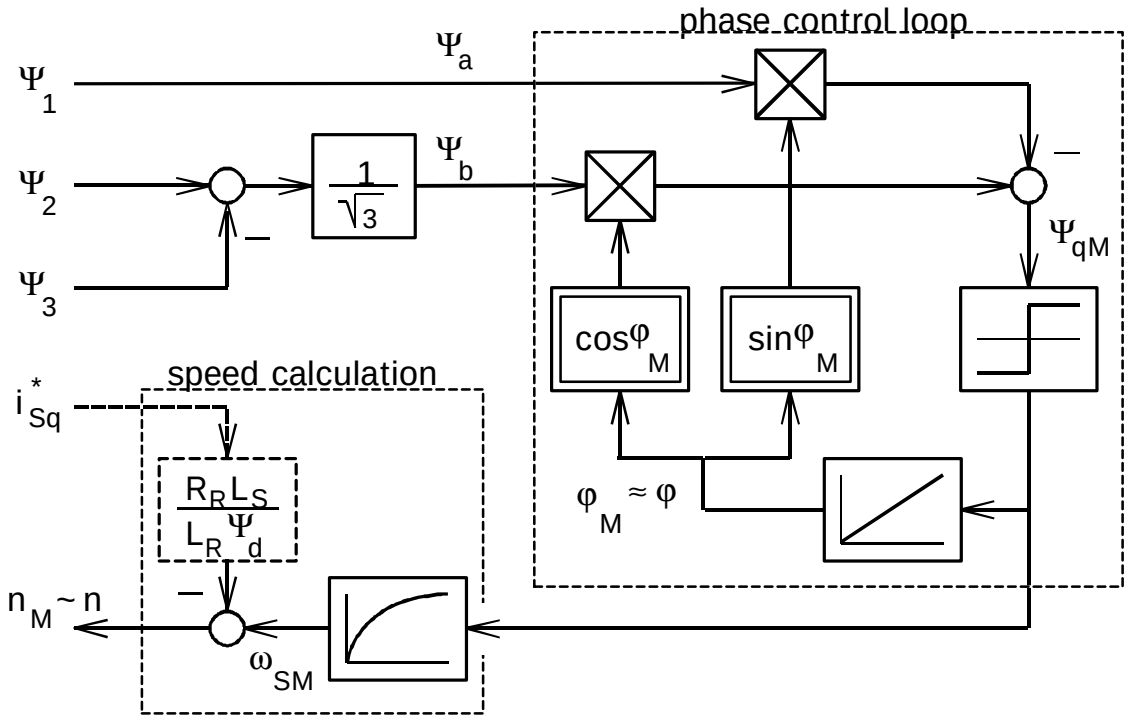

Figure 8: Flux identification by measuring φ, ω_S and n

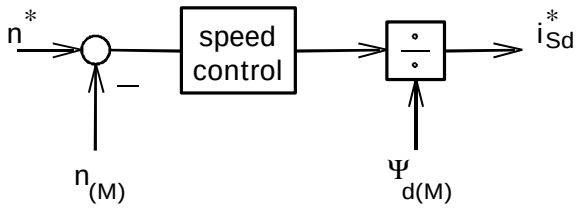

Figure 10: Decoupling the speed control loop from flux transitions

6. Problems in identifying the flux vector

Identifying the flux vector by integrating the stator voltages according to eq.(2) works very well at medium and higher stator frequencies and even with field weakening [8]. As long as the voltage drops across the stator resistors and the leakage inductances are small compared with the voltage induced by the flux, deviations of the machine's parameters from the parameters used in the flux calculation circuit have only a minor effect. However, at high stator frequencies and extreme field weakening the voltage across the leakage inductance is in the same order of magnitude as the voltage induced by Ψ_d. At very low stator frequencies the voltage across the stator resistors becomes even greater than the induced voltage. In these operating ranges the influence of mismatches between the actual parameters of the machine and of those parameters, used in the flux measuring circuit, must be considered.

6.1 Influence of the leakage inductance at very high frequencies

If there is a deviation in σL_S, the d-components used in the control algorithm are no longer in phase with the actual rotor flux of the machine. Nevertheless the torque still is

$$M_i \sim \Psi_d \cdot i_{Sq} - \Psi_q \cdot i_{Sd} = \Psi_d \cdot i_{Sq} \qquad (7)$$

and is directly controlled by i_{Sq}, because the phase control loop ensures, that $\Psi_q = 0$. But control actions of the speed control loop with i_{Sq} will now also cause transients of the flux Ψ_d [9]. If the leakage inductance σL_S was totally neglected in the flux model of eq.(2), the d-axis would be in phase with the stator flux instead of the rotor flux. To avoid any influence of flux transients on the machine's torque and the speed control loop, the simple decoupling measure shown in Fig. 10 may be used.

6.2 Influence of the stator resistors at very low frequencies

The flux integration of eq.(2) lies within the closed loops for Ψ_d and φ, so that drift effects, caused by operational amplifier offsets etc., are uncritical. However at very low speeds, the voltage drop across R_S becomes dominating and any mismatch between the real value and the value used in the flux calculation, which will especially be due to thermal effects, leads to phase and amplitude deviations in the measured flux values.

A first measure to reduce this effect is to control the low frequency gain of the integrators by a frequency dependent feedback $k(\omega_S)$. Fig.11a shows a possible realization. The integrating capacitor C is bypassed by resistor R_P, when switch S is closed, thus leading to a low pass filter instead of an integrator. To achieve a smooth transition to higher stator frequencies, where R_P is not needed, switch S is modulated with a duty cycle, which is dependent on the stator frequency. In combination with the inverter control scheme described in section 3, there is no need of additionally producing such a signal. The signal 'free wheeling' of the inverter's current control logic can be directly used, because 'free wheeling' will be very frequent at low stator voltages, i.e. low stator frequencies, and very seldom at high voltages, i.e. high stator frequencies.

A second measure is to use the flux model shown in Fig.1b instead of that in Fig.7. This model does only give the amplitude Ψ_d, not the angular position φ (Fig.11b). It has a limited dynamic accuracy and should not be used at higher stator frequencies, especially in the field weakening range, because it uses the time constant $T_R=L_R/R_R$, which is also extremely temperature dependent. But it is very well suited as an observer for backing the values, derived by the integrators, at low stator frequencies. To simplify the control circuit, the set value for i_{Sd} instead of the actual value is fed into the back up model. Again a smooth transition to higher frequencies is achieved by making the correction factor v dependent on ω_S.

At extremely low stator frequencies, when ω_S is much smaller than the nominal slip frequency $(s \cdot \omega_S)_N$, the phase control loop for φ may no longer ensure sinusoidal stator currents. For that operating range, the control structure is revised (Fig.12). Ψ_{qM} is controlled to zero by i_{Sq}^* with a second flux controller and the speed control acts directly on the input of the comparator of the phase control loop. A more advanced solution for this operating range, which also avoids a speed sensor, was presented in [10], but needs considerably more signal processing power, especially with inverters with high switching frequency. The same applies to methods trying to detect rotor speed utilizing slot harmonics [11].

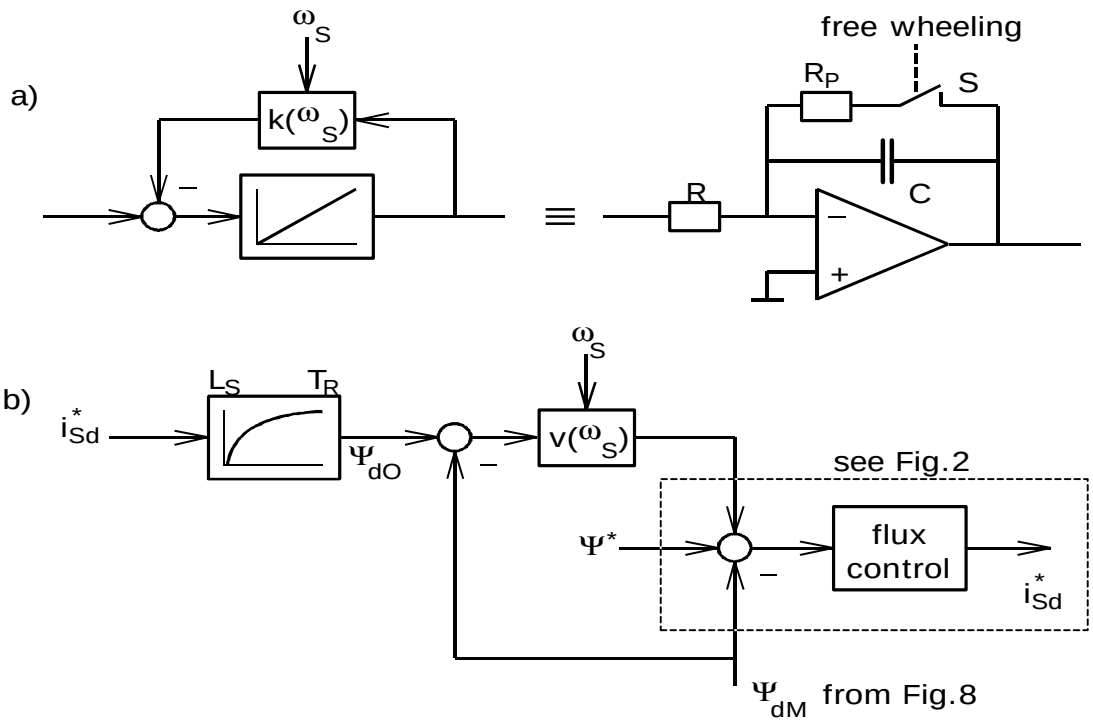

Figure 11: Improving the flux identification at low stator frequencies
a) stator frequency dependent 'integration' circuit
b) flux observer based on stator current instead of stator voltage

7. Conclusion and results

By using the amplitude and the angular position of the machine's flux a self controlled operation of the asynchronous machine is achieved, which does not need a speed or position sensor. The influence of the machine's electrical parameters on the control behaviour at medium and high stator frequencies is small. To improve the behaviour at low stator frequencies, the flux identification circuit, which integrates the stator voltages, is modified to make its low frequency gain dependent on the stator frequency. Additionally the flux controller is backed by a second flux model, which is based on the stator currents. Of course none of these measures ensures steady state operation of the drive with full torque at stator frequencies near zero, but it allows accelerating or deaccelerating a drive from and to standstill (Fig.13) and also guarantees very good performance, when stator frequency crosses through zero during speed reversal (Fig.14).

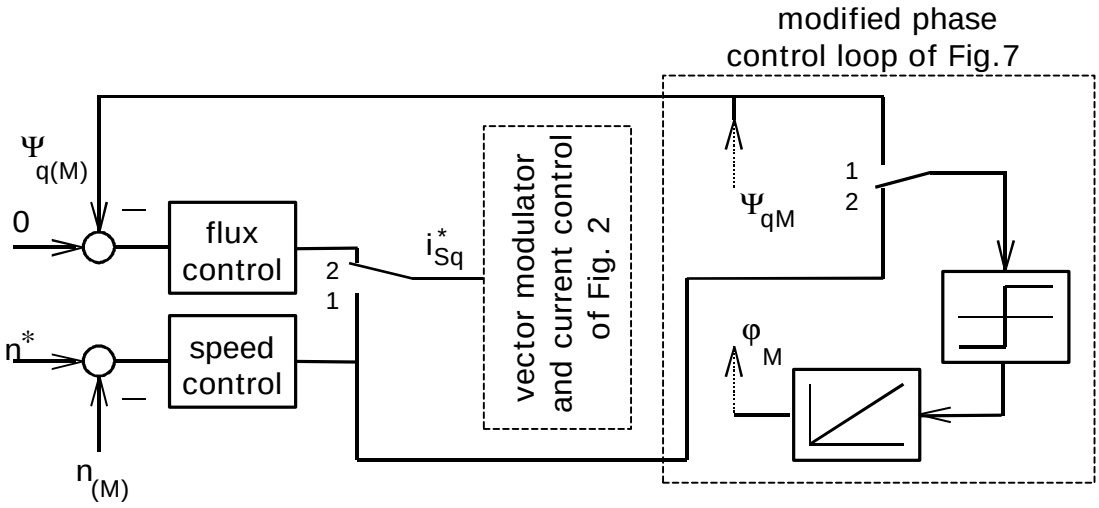

Figure 12: Revised control structure for extremely low stator frequencies
switch position 1: normal structure
switch position 2: revised structure

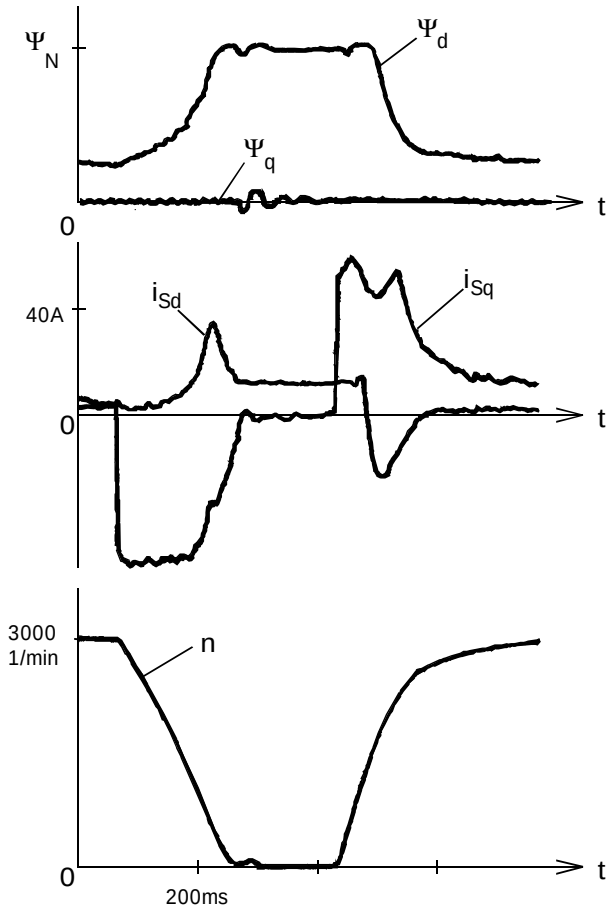

Figure 13: Speed profile including field weakening and standstill

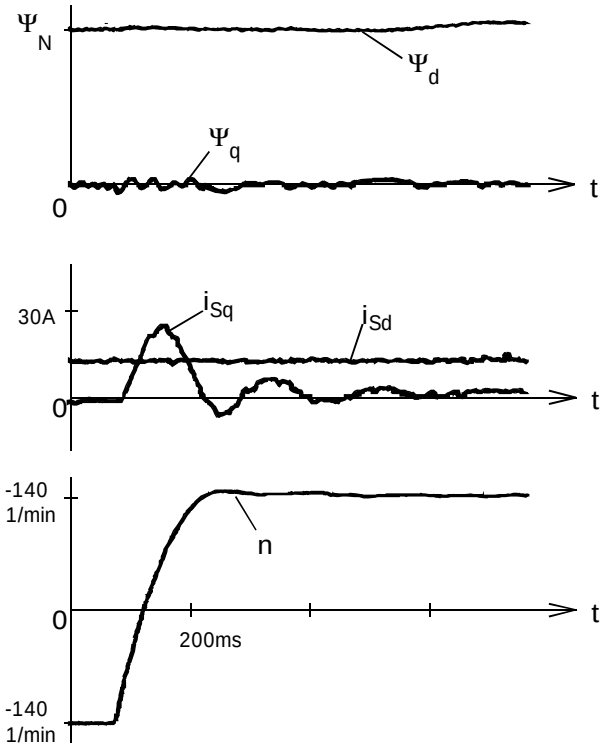

Figure 14: Speed reversal at low speeds

A. Appendix

Fig.13 and 14 refer to an AC machine with the following nominal data:

stator voltage	U_{SN} = 230 V
stator current	I_{SN} = 22 A
stator frequency	f_{SN} = 50 Hz
speed	n_N = 1445 min^{-1}
torque	M_{iN} = 73 Nm
moment of inertia	J_N = 0,05 $kg \cdot m^2$
stator resistance	R_S = 0,35Ω
leakage inductance	σL_S = 2 mH
rotor resistance	R_R = 0,46Ω
rotor inductance	L_R = 58 mH

References

[1] Boehringer, A.; Stute, G.; Ruppmann, C.; Würslin, R.: Entwicklung eines drehzahlgesteuerten Asynchronmaschinenantriebs für Werkzeugmaschinen. wt Zeitschrift für industrielle Fertigung,(1979) H.8, p.463-473

[2] Leonhard, W.: Control of electrical drives. Springer Verlag, 1985

[3] Depenbrock, M.: Direkte Selbstregelung (DSR) für hochdynamische Drehfeldantriebe mit Stromrichterspeisung. etzArchiv, (1985) H.7 . p.211-218

[4] Roth-Stielow,J.; Zimmermann,W.; Boehringer, A.; Schwarz,B.: Zwei zeitdiskrete Steuerverfahren für Pulsumrichter im Vergleich. etzArchiv (1989) H.12, p.389-396

[5] Roth-Stielow, J.: Beiträge zu Pulsumrichtersystemen großer Leistung mit nahezu sinusförmigen Ausgangsströmen hoher Frequenz. Dissertation Universität Stuttgart (1991)

[6] Deutsche Patentoffenlegungsschriften
DE 33 38 658, 1983; DE 34 07 741, 1984;
DE 40 03 453, 1990; DE 44 01 064, 1994

[7] Flett, F.P.: Vector control using a single vector rotation semiconductor for induction and permanent magnet motors. Technical publication, Analog Devices, 1992

[8] Joetten, R.; Schierling, H.: Control of the induction machine in the field weakening range. IFAC Control in Power Electronics and Electrical Drives, conference paper, Lausanne, Switzerland, 1983, p.297-304

[9] Bader, Uwe: Hochdynamische Drehmomentregelung einer Asynchronmaschine im ständerflußbezogenen Koordinatensystem. etzArchiv (1989) H.1, p.11-16

[10] Depenbrock, M.; Staudt, Volker: Determination of the stator flux space vector of saturated AC machines. etzArchiv (1990) H.11, p.349-351

[11] Haemmerli, B.M.: Rotor speed detector for induction machines utilizing slot harmonics.
ACEIM Conference, Turine, p.352-354